IOP Publishing Physica Scripta
Phys. Scr. 95 (2020) 044004 (11pp) https://doi.org/10.1088/1402-4896/ab635d

100 years of nuclear isomers—then and now

Philip Walker[1] **and Zsolt Podolyák**

Department of Physics, University of Surrey, Guildford GU2 7XH, United Kingdom

E-mail: p.walker@surrey.ac.uk and z.podolyak@surrey.ac.uk

Received 1 November 2019, revised 9 December 2019
Accepted for publication 18 December 2019
Published 13 February 2020

Abstract

The suggestion that some atomic nuclei would be able to exist in more than one stable or metastable configuration was proposed by Soddy in 1917. Subsequently, the first experimental example of such an isomeric pair was reported by Hahn in 1921, in the form of two metastable states of ^{234}Pa, then known as UZ and UX_2. Nowadays, of the 3437 nuclides listed in the most recent NUBASE evaluation, 1318 have at least one metastable excited state with a half-life of 100 ns or longer. The present work reviews historical aspects of nuclear isomers, and the different physical mechanisms that lead to their formation. Selected frontiers of contemporary isomer research are discussed, with an emphasis on remote regions of the nuclear landscape. Some possibilities for the electromagnetic manipulation of isomers are included.

Keywords: nuclear structure, isomeric states, atomic-nuclear interface

(Some figures may appear in colour only in the online journal)

1. Introduction

There are almost 300 different combinations of neutrons and protons (nucleons) that form the naturally occurring nuclides, i.e. the ones that are stable or have very long half-lives, so that they have survived on the Earth since its formation approximately 4.5 billion years ago. As atoms, with their surrounding electrons, these nuclides constitute the Earth itself and everything on it. In addition, there are thousands of nuclides with shorter half-lives, sometimes only fractions of a second, which can be synthesised and studied in the laboratory, and may have important uses such as in medical imaging and cancer treatment. Furthermore, every nuclide has excited states that arise from different arrangements of its given set of nucleons. The low-energy excited states typically are bound against nucleon emission, and most of them de-excite to the ground state rapidly by electromagnetic (γ-ray or conversion-electron) decay, on a time scale of picoseconds.

In contrast, nuclear isomers are relatively long-lived 'metastable' excited states, with half-lives ranging from nanoseconds to years. The existence of isomers depends on both the individual-nucleon orbits and the collective (whole nucleus) behaviour, so that empirical isomer properties shed light on these basic modes, and their interplay. The long half-lives of isomers can open up astrophysical applications, and more generally applications at the atomic-nuclear interface, including the possibility to achieve atomic manipulations of nuclear properties. A long-sought application would be the development of a γ-ray laser, and this goal could now be not far over the horizon.

Historically, the concept and manifestation of nuclear isomerism developed over several decades [1]. Initially, the hypothesis that there could exist two or more long-lived (or stable) states of a single nuclide was put forward by Soddy in 1917, who referred to states that are 'different in their stability and mode of breaking up', representing a 'finer degree of isotopy' [2], but it was not until 1921 that Hahn found the first example of an isomeric pair of states [3], UZ and UX_2, later known as ^{234}Pa and ^{234m}Pa (where the m specifies a metastable excitation). In fact, Hahn's new finding from a study of the β decay of ^{234}Th was the $T_{1/2} = 6.7$ h lowest-energy (ground) state of ^{234}Pa, while the 1.2 m decay from an excited state, which is the principal product of ^{234}Th β decay, had been identified eight years previously by Fajans and Göhring [4, 5].

Following Hahn's discovery, it turned out to be difficult to pin-down the details of the ^{234}Pa structure, and in 1934 Gamow suggested that the isomerism could be due to an antiproton in the nucleus [6]. Although he was far from the mark with his interpretation, Gamow seems to be the first to refer in the literature to 'isomeric' states, by analogy with chemical isomers, i.e. different physical arrangements of a

[1] Author to whom any correspondence should be addressed.

given set of constituents—atoms in the case of chemical isomers, protons and neutrons in the case of nuclear isomers. The following year, the production of neutrons through the bombardment of ^{9}Be by α particles [7, 8], enabled the discovery of further isomer examples, in indium and bromine [9, 10]. Then, in 1936, the explanation of isomers was given by von Weizsäcker in terms of spin (i.e. angular momentum) [11, 12]: large spin changes, especially when combined with low transition energies, could lead to low electromagnetic transition rates, and hence to the possibility of extended half-lives for excited states—the so-called spin isomers. These became a linchpin of the nuclear shell model [13–17]. The angular momentum could, in general, be understood as coming from unpaired nucleons: one nucleon in the case of low-energy states in odd-A nuclides (where A is the atomic mass number) and two nucleons in odd–odd nuclides. At higher excitation energies, broken pairs could generate substantial spin values. The existence of high-spin isomers at relatively low excitation energies gave rise to the term 'yrast traps', where the *yrast* (*dizziest*, from Swedish) states are those of lowest energy for a given spin.

It is worth noting that, following Soddy's suggestion (1917) and Hahn's discovery (1921), there remained considerable scepticism about the very existence of isomers, until von Weizsäcker's explanation (1936). Even von Weizsäcker remained doubtful, and is reported as saying (1936) that isomers 'in fact do not seem to occur' [18], just before he published his explanation of isomerism.

In 1937, Bethe published the second part of a nuclear physics review [19] with insightful comments about isomers. He considered that, at the time, bromine provided the best evidence for isomerism in nuclei. He also estimated that the mean partial γ-ray lifetime in units of seconds would be:

$$\tau = 5 \times 10^{-21} L!^{2} (20/E_{\gamma})^{2L+1}, \quad (1)$$

where L is the angular momentum carried by the emitted γ-ray photon and E_{γ} is its energy in MeV. It is now common practice to compare experimental half-lives with the Weisskopf single-particle estimates [20]. The following are the Weisskopf half-lives [21], in units of seconds, for dipole ($L = 1$) and quadrupole ($L = 2$) transitions:

$$T^{W}_{1/2}(E1) = 6.76 \times 10^{-15} E_{\gamma}^{-3} A^{-2/3}, \quad (2)$$

$$T^{W}_{1/2}(M1) = 2.20 \times 10^{-14} E_{\gamma}^{-3}, \quad (3)$$

$$T^{W}_{1/2}(E2) = 9.52 \times 10^{-9} E_{\gamma}^{-5} A^{-4/3}, \quad (4)$$

$$T^{W}_{1/2}(M2) = 3.10 \times 10^{-8} E_{\gamma}^{-5} A^{-2/3}. \quad (5)$$

The Weisskopf hindrance factor can then be expressed as:

$$F_{W} = T^{\gamma}_{1/2} / T^{W}_{1/2}, \quad (6)$$

where $T^{\gamma}_{1/2}$ is the partial γ-ray half-life, which is determined experimentally.

The 1930s were key years for nuclear physics, leading to Hahn and Strassmann's observation of barium after bombarding uranium with neutrons (published early in 1939) [22]; and Meitner and Frisch's explanation in terms of the fission of uranium [23]. Meitner, in particular, had been advocating that isomers were key to understanding the many different half-lives that were being observed when bombarding uranium with neutrons, perhaps significantly delaying the discovery of fission itself. So, they are telling words in the 1939 paper: '... it might not be necessary to assume nuclear isomerism' [23]. This did not, of course, stop a growing interest in the role of isomers in nuclear structure.

The realisation that nuclei could be non-spherical opened the way to their description in terms of deformed shapes with axial symmetry, and hence, in 1955, to the specification of the K quantum number and K-forbidden transitions [24]. Here, K is the projection of the total angular momentum, I, on the symmetry axis. Due to incomplete conservation of K, these K-forbidden transitions were already understood to be inhibited rather than strictly forbidden, and the degree of K forbiddenness of a transition was expressed as $\nu = \Delta K - L$, where ΔK is the change in K (see also section 4). Therefore, while von Weizsäcker [11] had focussed on the role of the magnitude of the angular momentum, a nuclear symmetry axis meant that the direction of the angular momentum vector could also be important, leading to the formation of K isomers.

In fact, K isomers had been observed even before the K quantum number was known to exist. The first cases with (later understood to be) highly K-forbidden decays were in ^{190}Os (1950) [25] and ^{180}Hf (1951) [26]. The latter is particularly notable because of Bohr and Mottelson's interpretation (1953) [27] of the near-perfect rotational character of the states populated in the isomer's decay. The (later) structural understanding of K isomers depended to a significant extent on the rotational character that they had themselves revealed.

A third class of isomers was discovered in 1962 by Polikanov *et al* [28, 29]. They found isomeric fission from a $T_{1/2} = 14$ ms excited state of ^{242}Am, which could be interpreted as being due to a superdeformed minimum in the potential-energy surface [30, 31]. Fission isomers have been found with nucleon numbers $90 \leqslant Z \leqslant 97$ and $141 \leqslant N \leqslant 151$ [30–32] and fall within the broader class of 'shape isomers' [33]. The inhibition of the decay transitions comes from the associated shape changes, which involve substantial configuration changes, i.e. changes in the individual nucleon orbits. The longest-lived shape isomer is the 14 ms ^{242}Am fission isomer.

The three principal classes of isomerism, due to changes in spin, K and shape, can occur in any combination, though the decay inhibition due to a shape change can be difficult to recognise and separate from spin- and K-changing influences. An unambiguous example of a mixture of spin and K isomerism is evident in the 2.5 MeV, $I^{\pi} = K^{\pi} = 16^{+}$ isomer of ^{178}Hf (π is the parity). Here, the predominant electromagnetic decay [34] is by a 13 keV, $\Delta I = 3$, $E3$ transition (low energy, high multipole order) with $\Delta K = 8$, hence with large K-forbiddenness, $\nu = 5$. The resulting half-life from the combination of both spin and K isomerism is 31 years. (Note that, in deformed nuclei, the K value for an isomer is almost always assumed to be equal to its spin, I.) From the historical perspective, the $K^{\pi} = 10^{-}$, 16 m isomer of ^{182}Ta should also be mentioned. Discovered in 1947 [35], it is the earliest example

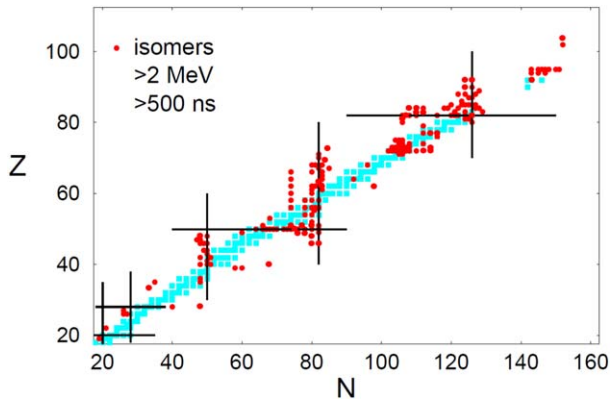

Figure 1. Nuclear chart of proton number, Z, versus neutron number, N, showing isomers (red dots) with excitation energies greater than 2 MeV and half-lives geater than 500 ns. Naturally occurring nuclides are represented as pale blue squares. The black lines are at the magic numbers where shell gaps favour spherical shapes.

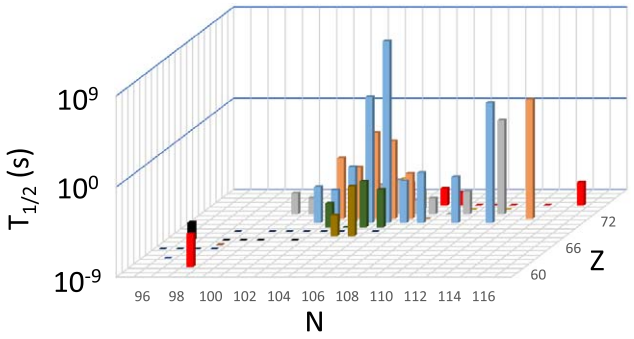

Figure 2. Representation of isomer half-lives in the deformed rare-earth region ($60 \leqslant Z \leqslant 76$, $96 \leqslant N \leqslant 116$) where each isomer involves at least four unpaired nucleons. For a given nuclide with more than one such isomer, the maximum half-life is illustrated. Each value of Z is represented by a given colour, e.g. blue for $Z = 72$ (hafnium). The data are from Kondev *et al* [38], except for the lowest-mass example, ^{160}Sm [39]. Naturally occurring nuclides are shown as squares in the N–Z plane.

that has $\nu > 1$, K-forbidden decay, though its long half-life comes more from the high multipole order, $E3$, of its predominant decay branch [36], rather than the weak ($\nu = 2$) degree of forbiddenness—making it more of a spin isomer than a K isomer.

Considering the whole nuclear chart, with 3437 nuclides listed in the most recent NUBASE evaluation [37], 1318 have at least one isomer with a half-life of 100 ns or longer. They are distributed over the whole mass range, from $^{12}_{4}$Be (2251 keV, $T_{1/2} = 229$ ns) to $^{270}_{110}$Ds (1390 keV, $T_{1/2} = 10$ ms). Although widespread, the distribution of isomers is far from being random. Figure 1 shows this effect for isomers with excitation energies greater than 2 MeV and half-lives greater than 500 ns. It is evident that the isomer-favoured nucleon numbers cluster around closed shells, but there are also groups of isomers well away from the closed shells, in regions of prolate (rugby-ball shaped) deformation. These are mostly high-K isomers. A different representation is shown in figure 2 for high-K isomers involving at least four unpaired nucleons, in the $A \approx 180$ deformed region, with ^{178}Hf providing the longest half-life of 31 years ($\approx 10^9$ s).

The 100 ns lower limit for specifying an isomer in the NUBASE evaluation [37] is arbitrary. Indeed, the use of the term 'isomer' depends on the context and has changed over the years. Experimentally, a key point is that isomeric-state half-lives can enable the separation in time and/or space of the decay radiations, from the usually much more intense 'prompt' radiation flux emitted within picoseconds of the production process. On this basis, one of the shortest-lived isomers is a fission isomer of ^{240}Cm, with a half-life of 10 ps [40]—sufficient time to identify delayed-fission events. More typically, for γ-ray measurements, a half-life of a few nanoseconds is needed.

At the other end of the half-life range, there is only one quasi-stable isomer, ^{180m}Ta, which is a 75 keV, $K^\pi = 9^-$ excitation. It could, in principle, decay by 75 keV, $M8$ ($\nu = 0$) and 35 keV, $E7$ ($\nu = 1$) electromagnetic transitions, but these have not been observed and the current half-life limit is $T_{1/2} > 4.5 \times 10^{16}$ years [41]. Meanwhile, the ground state has a half-life of 8 h. Thus, uniquely, the isomer exists naturally, but not its ground state. There is no known nuclide where both the ground and isomeric states are naturally occurring.

The energies of isomers in deformed nuclei range from 8.3 eV for a $K^\pi = 3/2^+$ state in ^{229}Th [42] with $T_{1/2} = 7\ \mu$s [43], to 7.5 MeV for a $K^\pi = 57/2^-$ state in ^{175}Hf with $T_{1/2} = 22$ ns [38, 44], though, for the identification of higher isomer energies, it could be experimental access that is the main limiting feature. In spherical or near-spherical nuclei, the highest-energy isomer known is an $I^\pi = 28^-$ state in ^{208}Pb at 13.8 MeV, with $T_{1/2} = 60$ ns [45].

In addition to electromagnetic decay, isomers can decay by the same processes as ground states, namely α decay, β decay, fission and proton decay. Indeed, proton radioactivity was first observed from an isomer, ^{53m}Co [46, 47]. It could be that neutron radioactivity will, at some future date, be first identified from an isomer [48–50].

Leading on from earlier work [51–55], there have been several recent reviews of isomers. Jain *et al* [56] listed all isomers with half-lives greater than 10 ns, compared to the 100 ns lower limit in the NUBASE evaluation [37]; Heyde and Wood have discussed shape coexistence and shape isomerism [33, 57]; Kondev *et al* [38] made a comprehensive analysis of high-K isomers with mass number $A > 100$, excluding one-particle isomers in odd-A nuclides and two-particle isomers in odd–odd nuclides; Walker and Xu [58] discussed K isomers and their rotational structures; Dracoulis *et al* [59] reviewed all high-spin isomer structures for $A > 150$, including discussion of experimental techniques, and medical and other applications (note that the most commonly used radionuclide for medical imaging is itself an isomer, ^{99m}Tc); and Ackermann and Theisen [60, 61] summarised the data on K isomers in superheavy nuclei.

2. Shape and fission isomers

Fission isomers were first observed by Polikanov *et al* [28, 29] in 1962, and their discovery sparked an intense period of investigation, with associated reviews [30–32, 62–65]. The delayed fission enabled highly sensitive experiments to be performed, with half-lives down to 10 ps [40]. The theoretical understanding hinged on the incorporation of shell effects into the liquid drop model [31, 66, 67]. The fission takes place from a second minimum in the potential-energy surface, with superdeformed shape (prolate spheroid, with axis ratio 2:1) and $I^{\pi} = 0^{+}$ in the case of even–even nuclei. Two examples of fission isomers have been found where γ-ray 'back-decay' to states in the first well competes with spontaneous fission, namely ^{236}U [68] and ^{238}U [69]. Here, γ-ray back-decay can be viewed as shape-tunnelling through the axially symmetric quadrupole (β) shape degree of freedom—see also section 4 for comparison with *K*-isomer decay by tunnelling through the γ degree of freedom. Fission isomer properties, including half-lives, are broadly understood in terms of the underlying shell structure [70–73], with new advances for odd-*A* nuclides [74]. A recent experiment identified a $T_{1/2} = 3.6$ ms fission isomer in ^{235}U for the first time [75].

Isomeric excitations within the second well were also found, such as in ^{238}Pu [76], where the more highly excited isomer has a longer half-life. This is interpreted as a high-*K* isomer in the second well, a situation recently discussed by Liu *et al* [77]. In common with the other examples, it is not known whether the high-*K* 'fission' isomer actually fissions, or whether it γ decays to the ground state of the second well and then fissions.

Fission isomers are examples of the more general class of shape isomers [33, 57, 78]. Often, different shapes coexist without isomerism being evident, as exemplified in ^{186}Pb, with three different $I^{\pi} = 0^{+}$ states identified below 1 MeV [79]: the ground state together with excited states at 532 and 650 keV, having spherical, oblate and prolate shapes, respectively. Even when isomeric, $I^{\pi} = 0^{+}$ excitations are short lived, with $T_{1/2} < 3\,\mu$s throughout even–even nuclei [56].

It is interesting to consider the situation in even–even nuclei where an $I^{\pi} = 0^{+}$ isomer is the first excited state. In that case, single-photon decay to the $I^{\pi} = 0^{+}$ ground state is forbidden, and there is enhanced sensitivity to two-photon decay, in competition with $e^{+}e^{-}$ pair decay and conversion-electron decay. There has been successful observation of two-photon decay in ^{16}O, ^{40}Ca and ^{90}Zr, in each case with a branching ratio between 10^{-4} and 10^{-3} [80]. If, in addition, the $I^{\pi} = 0^{+}$ isomer has an excitation energy below 1022 keV, then $e^{+}e^{-}$ pair decay is no longer possible. Recently, Henderson *et al* [81] set a branching ratio limit of $<10^{-4}$ for ^{98}Mo, where the 0^{+} isomer is at 735 keV. Now consider producing this kind of isomer in a storage ring [82] with all the electrons removed, so that conversion-electron decay is impossible: the half-life would increase by several orders of magnitude, and it may be possible to study two-photon decay (and perhaps other rare processes) simply by measuring the value of the extended half-life. There are only four nuclides with 0^{+} isomers ($T_{1/2} > 10$ ns) where this opportunity exists: ^{72}Ge, ^{72}Kr, ^{98}Zr and ^{98}Mo.

Shape isomerism may be combined with spin and/or *K* isomerism, though the relative importance of the different transition-inhibition mechanisms is difficult to separate. An outstanding example is the triple coexistence, within 240 keV, of three isomers in ^{188}Pb [33, 59, 83]: a prolate $K^{\pi} = 8^{-}$ isomer at 2577 keV with $T_{1/2} = 1.2\,\mu$s; an oblate $K^{\pi} = 11^{-}$ isomer at 2702 keV with $T_{1/2} = 38$ ns; and a spherical $I^{\pi} = 12^{+}$ isomer at 2710 keV with $T_{1/2} = 136$ ns. Longer-lived isomers associated with substantial shape differences have been identified from their mean-square charge radii measured by laser hyperfine spectroscopy [84], such as ^{98m}Y with $T_{1/2} = 2$ s, and ^{185m}Hg with $T_{1/2} = 22$ s. In these examples, substantial spin differences, between isomer and ground state, are also involved.

3. Spin and seniority isomers

The lifetime of an excited nuclear state is determined by the properties of the possible decay paths, and depends very strongly on the angular momentum (*L*) of the de-exciting photons. For non-parity-changing transitions, typical emission probabilities have ratios for $L = 1(M1):L = 2(E2):L = 3(M3):L = 4(E4)$ of $1{:}10^{-3}{:}10^{-10}{:}10^{-13}$. Corresponding values for parity-changing transitions are $1{:}10^{-7}{:}10^{-10}{:}10^{-17}$ [85]—see also equations (2)–(5). In addition, for a fixed *L* the partial half-life is given as $T_{1/2} \sim 1/(E_{\gamma})^{2L+1}$. Consequently, long-lived isomeric states are expected when the available decay paths require high *L* and/or low E_{γ}. At low E_{γ} the competing decay via internal electron conversion becomes important, which can greatly reduce the $T_{1/2}$ dependence on energy.

As an example of spin isomers, the isotopic chain of neutron-rich odd-mass gold isotopes is presented. The structure of ^{205}Au with a magic number of neutrons, $N = 126$, is characterised by single-proton-hole states. There are only two states expected below the $I^{\pi} = 11/2^{-}$, $h_{11/2}$ excited state at 907 keV [86]: the $3/2^{-}$, $d_{3/2}$ ground-state and the so-far unidentified $1/2^{-}$, $s_{1/2}$ state. Therefore, the minimum spin change of the decay is $11/2 - 3/2 = 4\,\hbar$, which results in a seconds-long lifetime [86]. In contrast, in the lighter ^{203,201,199}Au isotopes [87–90], a $7/2^{+}$ state is also present below the $11/2^{-}$ state, opening a decay path with $L = 2$. This reduces the lifetime by several orders of magnitude. Nevertheless, the $11/2^{-}$ states remain isomeric, due to the low $L = 2$ decay energies. In ^{197}Au [91], the situation is somewhere between that in ^{205}Au and ^{203,201,199}Au. The available state between the $11/2^{-}$ state and ground state has spin-parity $5/2^{+}$, therefore the decay from the isomer proceeds via a low energy *E*3 transition. This results again in a much longer half-life, similar to that in ^{205}Au. The evolution of the $11/2^{-}$ isomeric states in $^{197–205}$Au, shown in figure 3, provides a good illustration of the importance of both *L* and E_{γ}.

In the above discussion we did not consider the wave functions of the states involved. Transitions between states

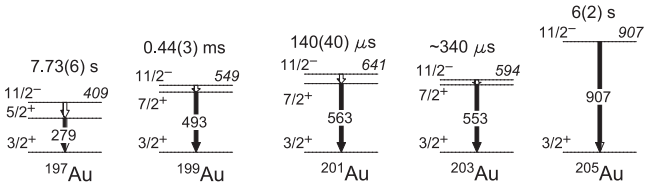

Figure 3. Spin isomers in the $^{197-205}$Au odd-mass isotopic chain [86–91]. Transition energies and isomer excitation energies (in italics) are in keV, and the isomer half-lives are given.

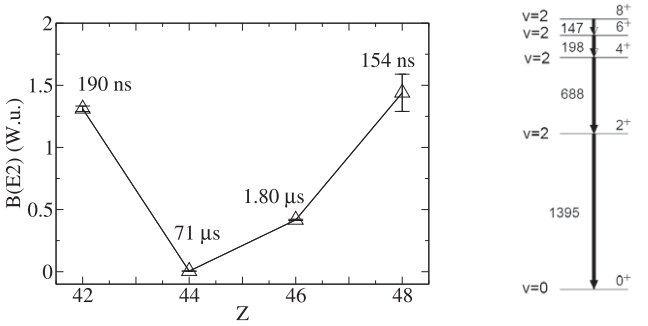

Figure 4. Reduced transition strengths in Weisskopf units, W.u. $= 1/F_W$, for the 8^+ isomeric states in the $N = 50$ isotones ^{92}Mo, ^{94}Ru, ^{96}Pd, and ^{98}Cd [95–97]. The isomer half-lives are given. The characteristic U shape is clearly visible, although it is not quite symmetrical. On the right-hand side, as an example, the level scheme of ^{98}Cd [98] is shown, with the seniority numbers given for each state.

can be inhibited because of nuclear structure reasons. One such case is that of seniority isomers.

The term seniority was introduced by Racah in the context of electrons in order to explain atomic spectra [92]. In nuclear physics, seniority (denoted by the letter v) is the number of nucleons that are not paired to angular momentum zero. Seniority isomers occur in semi-magic nuclei. In the ground-state of an even–even nucleus the seniority is zero, i.e. all nucleons are paired to angular momentum zero. The lowest energy excited states are formed by breaking a proton or neutron pair, therefore they have seniority $v = 2$. A classic example of seniority isomers is in the $N = 50$ isotones with $Z = 42$–48: ^{92}Mo, ^{94}Ru, ^{96}Pd, ^{98}Cd. The two unpaired protons are in the $g_{9/2}$ orbital and the $v = 2$ states have angular momenta $I = 2, 4, 6, 8$. The 8^+ states are isomeric due to the low energy of the $8^+ \rightarrow 6^+$ electric quadrupole $E2$ transition. In addition, the reduced transition strength, $B(E2)$, is small when the valence $g_{9/2}$ orbital is close to being half filled. This is because the quadrupole operator is zero at mid-shell [93]. The characteristic U-shaped transition strength curve is shown in figure 4, together with the level scheme of ^{98}Cd. Note that the seniority isomers do not involve a change in seniority. The isomer and the state it decays to have the same seniority. In contrast, the $B(E2)$ of the seniority-changing $\Delta v = 2$ transitions, such as the $2^+ \rightarrow 0^+$ transition, has an inverted U shape as a function of Z, with the maximum at mid-shell [94].

While the previous case involves protons in the $g_{9/2}$ orbital, $g_{9/2}$ neutrons give rise to similar 8^+, $v = 2$ seniority isomers. This is the case in neutron-rich semi-magic ($Z = 82$) lead isotopes. As expected for seniority isomers, the transition

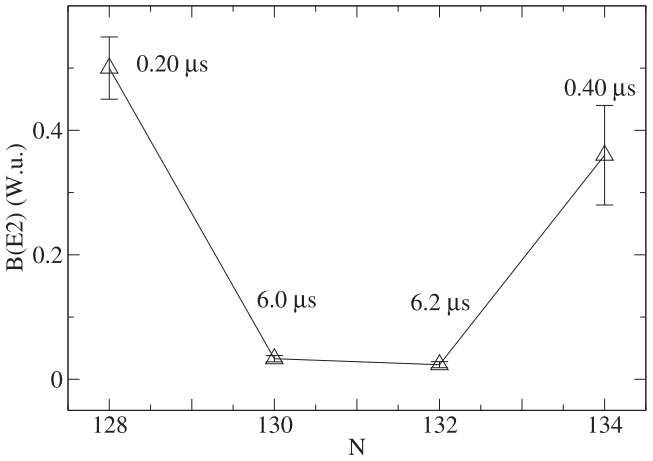

Figure 5. Reduced transition strengths for the 8^+, neutron $g^2_{9/2}$ states in the $^{210-216}$Pb isotopes [99, 100]. The isomer half-lives are given. The characteristic U shape is clearly visible, although it is a little distorted.

strength of the $8^+ \rightarrow 6^+$ decay is larger when either the $g_{9/2}$ orbital is almost empty (^{210}Pb) or almost full (^{216}Pb), with the minimum when the orbital is roughly half full (^{212,214}Pb) [99]. This is illustrated in figure 5.

Neither in the $N = 50$ nor in the $Z = 82$ chains is the variation in the transition strength from the isomeric states perfectly symmetric. For example $B(E2;\ ^{94}\text{Ru}) < B(E2;\ ^{96}\text{Pd})$, and $B(E2;\ ^{210}\text{Pb}) > B(E2;\ ^{216}\text{Pb})$. These variations are explained by a more complex structure of the two states involved, that of the isomer and the state it decays to. In the lead isotopes, the higher lying $i_{11/2}$ neutron orbital also gives rise to 8^+ and 6^+ states. These mix with the neutron $g^2_{9/2}$ states, and the perfect symmetry in $B(E2)$ is destroyed. The $B(E2)$ values in all four isotopes have been explained quantitatively by considering effective three-body interactions [99] in the shell model. An often invoked effect is seniority mixing. Higher seniority states with $v = 4$ can mix with the $v = 2$ states of the same spin-parity. However, the mixing matrix element is small compared to the typical energy difference between $v = 2$ and $v = 4$ states, usually resulting in only small seniority mixing, as shown by Van Isacker [101].

Seniority isomers are expected, and have been observed, involving other high-j orbitals as well. For example, in the neutron-rich $Z = 50$ tin isotopes the $f_{7/2}$ neutron orbital is the first one to be filled beyond doubly magic ^{132}Sn. Indeed, the 6^+ states with an $f^2_{7/2}$ configuration are isomeric in ^{134,136,138}Sn [102]. However, the $B(E2)$ does not exhibit the expected U-shaped behaviour (see figure 6). The transition strength decreases as neutrons are added to the $N = 82$ closed shell. The $B(E2)$ at ^{136}Sn is large, while based on the seniority scheme it should be zero. The experimental value can be reproduced by reducing the neutron $f^2_{7/2}$ matrix elements. This has the effect of lowering the energy of the second 4^+ ($v = 4$) state, so that it lies close to the first 4^+ ($v = 2$) state and there is strong mixing between them. If the yrast 4^+ state has roughly equal parts of $v = 2$ and $v = 4$ components, the high $B(E2)$ value is reproduced [102]. (Recall that the $\Delta v = 2$ transition strengths are maximal when the orbital is half full.)

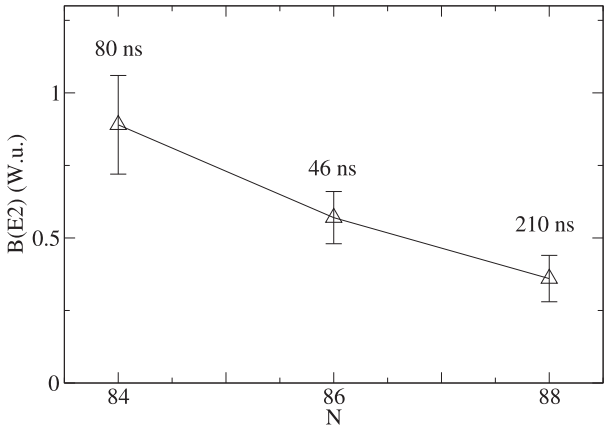

Figure 6. Reduced transition strengths for the 6^+ isomeric states in ^{134,136,138}Sn [102, 103]. The isomer half-lives are given. The simple seniority scheme is not valid.

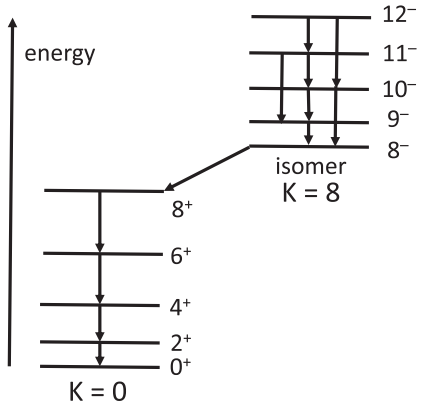

Figure 7. Conceptual diagram of some excited states in a deformed, axially symmetric, even–even nucleus. Here, a $K^\pi = 8^-$ isomer decays into the rotational band built on the $K^\pi = 0^+$ ground state. Rotational states built on the isomer are also shown. In this example, the isomer decays by an $8^- \rightarrow 8^+$, $E1$ transition with $\Delta K = 8$ (angled arrow).

A slightly different behaviour has been observed in the neutron-rich $Z = 28$, $^{70-76}$Ni isotopes. Here the 8^+ states have the neutron $g^2_{9/2}$ configuration. Close to mid-shell, in ^{72}Ni the $B(E2)$ value is surprisingly large, practically destroying the isomerism [104]. The case is similar in ^{74}Ni. This was explained, for both nuclei, by the predicted presence of closely spaced 6^+ states with seniority $v = 2$ and $v = 4$. The 8^+, $v = 2$ state decays into the 6^+, $v = 4$ state with large $B(E2)$ [101].

The departure from the expected U shape of the $B(E2)$ transition strengths can also be explained within the formalism of the generalised seniority scheme. This concept was introduced by Arima and Ichimura [105] for multi-j orbits, i.e. several orbitals with different total angular momentum. Recently this was developed further and successfully applied for several cases. For the $^{134-138}$Sn nuclei discussed above, considering multi-j degenerate orbitals, the observed trend was reproduced [106]. The generalised seniority method is consistent with the more sophisticated shell-model calculations.

Higher seniority isomers also exist. For example, in the tin isotopic chain, $v = 4$ isomers are known in a range of nuclei below ^{132}Sn, with tentative $v = 6$ isomers also identified [107]. The odd-mass tin isotopes exhibit $v = 3$ seniority isomers [108]. All these isomers in both the even- and odd-mass tin isotopes involve the high-j, neutron $h_{11/2}$ orbital. Due to the low number of particles involved, the shell model is the natural tool for the theoretical studies. The generalised seniority scheme has also been used successfully to describe seniority isomers with $v = 2$ and $v = 4$ in the tin isotopes, including their $E1$ decays [109].

In the above, the focus has been on reduced transition rates, as these provide sensitive probes of the model wave functions. For nuclei close to shell closures, the shell model is also successful with excited-state energy calculations, but these are less discriminating.

Isomeric states can be used as a tool to increase the sensitivity of experiments. Nuclei produced with very low yield can be physically separated from others and their decay properties studied. In several cases the most exotic, neutron-rich isotopes have been studied in this way, as was the case in the above-mentioned lead and tin isotopic chains. A good example for future work is the study of neutron-rich $N = 126$, $Z < 82$ isotones. The even–even isotones are expected to have a 10^+ seniority isomer with the proton $h^2_{11/2}$ configuration. These were already identified in ^{206}Hg [110] and ^{204}Pt [111]. Isomerism is expected to persist in the lighter isotones as well, providing a gateway for their experimental study. The understanding of these neutron-rich nuclides is essential for refining the theoretical predictions of the properties of the astrophysical r-process waiting-point nuclides along the $N = 126$ closed shell. In contrast, some of the r-process waiting-point nuclides along the $N = 82$ closed shell were already synthesised and studied experimentally. This could be achieved for ^{130}Cd [112] and ^{128}Pd [113] due to the existence of the $v = 2$, 8^+ seniority isomers with the proton $g^2_{9/2}$ configuration. Equivalent isomeric states are expected for lighter isotopes as well.

The isomeric states in the r-process path nuclides are important not only because they provide extra sensitivity for their study. They can also influence the nucleosynthesis itself [114]. In nucleosynthesis environments, the isomers can be populated thermally, and they can also be fed via neutron capture. The effective lifetimes of individual nuclides can therefore be modified, ultimately affecting the yields of the r-process elements.

4. *K* isomers

As already outlined in section 1, K isomerism arises in deformed nuclei that have so-called 'K-forbidden' transitions, which are inhibited rather than strictly forbidden. The level structure associated with a typical K isomer is illustrated schematically in figure 7. Note that the isomer decay proceeds through the transition of lowest possible multipole order, $L = 1$, although it has a high degree of K forbiddenness, $\nu = \Delta K - L = 7$. The nuclide ^{178}Hf (for example) has a

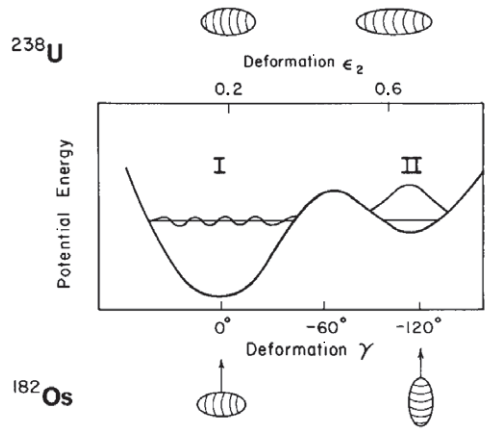

Figure 8. Schematic representation comparing K-isomer decay in ^{182}Os by tunnelling through the γ degree of freedom, with shape isomer back-decay in ^{238}U, from Chowdhury *et al* [128]. ($\epsilon_2 \approx 0.95\beta_2$.)

$K^\pi = 8^-$ isomer of this type, with a half-life of 4 s [37] for its $E1$ decay. As a rule of thumb, the transition-rate inhibition is approximately a factor of 100 per degree of K forbiddenness [115–117], expressed as $f_\nu \approx 100$, where f_ν is the reduced hindrance. More specifically, $f_\nu = F_W^{1/\nu}$, where F_W is the Weisskopf hindrance factor, as defined in equation (6). Although the Weisskopf transition rates, and hence the hindrance factors, are simple approximations, this formulation seeks to take into account the transition energy, multipole order and K-forbiddenness, so that any variations in f_ν should depend on K-mixing processes and the associated nuclear structure.

Reduced-hindrance values can vary widely, both between and within nuclides. Compare, for example, the $\nu = 7$, $E1$ decay of the ^{178}Hf, $K^\pi = 8^-$ isomer which has $f_\nu = 79$, with the $\nu = 2$, $E2$ decay from a $K^\pi = 6^+$ isomer in the same nuclide with $f_\nu = 5$ [38]. Evidently, there are large differences in K mixing that need to be understood [38, 55, 59]. With this objective, the principal K-mixing mechanisms can be characterised as rotational (Coriolis) mixing [118–120]; shape tunnelling through the triaxial (γ) degree of freedom [121–123]; statistical mixing due to level-density effects [58, 124, 125]; and chance near-degeneracies [126, 127]. However, it is difficult to disentangle these different contributions to K mixing, and a unified treatment remains to be established.

Consider, for example, the γ-tunnelling approach. Chowdhury *et al* [128] proposed that K-isomer decay could involve tunnelling through the γ degree of freedom in the potential energy surface, from $\gamma = -120°$ (prolate non-collective) for the isomer itself, directly to $\gamma = 0°$ (prolate collective) in the ground-state band. Such a decay mode is illustrated in figure 8, where the γ-tunnelling decay of the $K^\pi = 25^+$ isomer of ^{182}Os is compared with the axially symmetric ($\gamma = 0°$) tunnelling involved in the back-decay of the superdeformed shape isomer of ^{238}U. Both types of tunnelling decay correspond to shape transitions where the orientation of the bulk matter remains fixed [119].

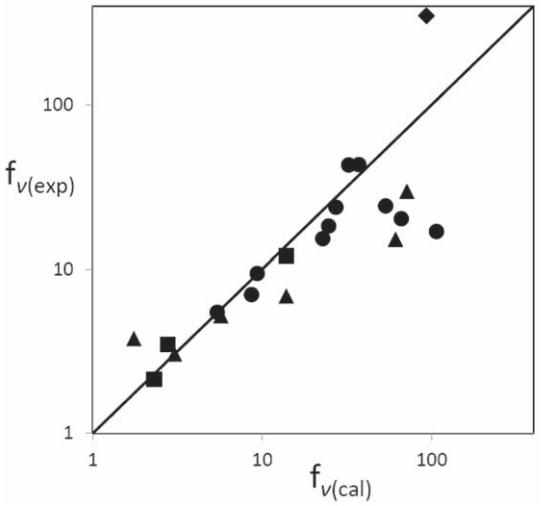

Figure 9. Comparison between γ-tunnelling estimates of $E2$ reduced-hindrance factors, $f_{\nu(\mathrm{cal})}$, and the corresponding experimental values, $f_{\nu(\mathrm{exp})}$, for $Z = 70$ (diamond), 72 (circles), 74 (triangles) and 76 (squares) high-K isomers. Equal calculated and experimental values would lie on the diagonal. Most of the theoretical values are from Narimatsu *et al* [122], replotted in terms of f_ν values, with the K-forbiddenness, ν, taken from Kondev *et al* [38] (and $K = 7$ is assumed for the 2685 keV level of ^{174}Hf [131]). The experimental values are from Kondev *et al* [38]. Additional theoretical values are included for ^{174}Yb [129], which has the highest value of $f_{\nu(\mathrm{exp})}$, and for ^{174}W [130], which has the lowest value of $f_{\nu(\mathrm{cal})}$. Experimental uncertainties are smaller than the data points.

Building on the work of Bengtsson *et al* [121], systematic γ-tunnelling calculations of $M1$ and $E2$ transition rates from hafnium ($Z = 72$), tungsten ($Z = 74$), and osmium ($Z = 76$) isomers were carried out by Narimatsu *et al* [122] (see also Crowell *et al* [123]). The same methodology was later used to include the $K^\pi = 6^+$ isomer decay of ^{174}Yb [129] and the $K^\pi = 12^+$ isomer decay of ^{174}W [130], and all the results for $E2$ reduced hindrance factors are shown in figure 9.

Overall, the agreement between these calculated and experimental $E2$ reduced-hindrance factors is good, especially considering that there is a large spread of values. Nevertheless, other degrees of freedom are likely to be involved, which could explain why some of the experimental reduced hindrances fall below the diagonal line of figure 9. However, the experimental hindrances for the ^{174}Yb [129] and ^{174}W [130] isomers lie significantly above the diagonal, and these cannot be understood within the γ-tunnelling model.

Despite difficulties with the interpretation of K-forbidden transition rates, it is relatively straightforward to calculate K-isomer energies in terms of unpaired nucleon orbits [132–134]. For example, the experimental and calculated energies of high-K states in ^{178}W [133, 135], up to $K = 34$, are illustrated in figure 10. The configuration-constrained calculations use a deformed Woods–Saxon potential with Strutinsky shell correction and Lipkin–Nogami pairing [133]. It is evident that the differences between the calculated and experimental energies increase with angular momentum. However, as a percentage, these differences are approximately

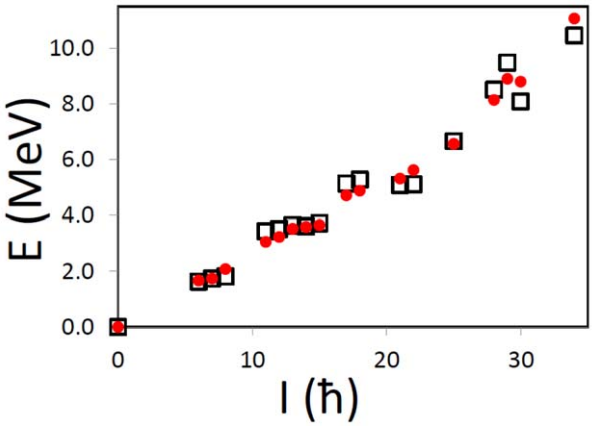

Figure 10. Energy as a function of angular momentum for high-K states in ^{178}W, with values taken from [133, 135]. Filled red circles represent the experimental data, and open black squares are from configuration-constrained calculations. Experimental uncertainties are smaller than the data points.

spin-independent, averaging 1.7% (rms value, excluding the ground state).

The wide-ranging success of such calculations for understanding K-isomer excitation energies, especially calculations that take into account the possibility that each excited configuration can have separately determined deformation parameters (β_2, γ, β_3, β_4, β_6) [133, 136, 137] leads to their use to predict favoured K-isomer regions that have not yet been adequately explored experimentally. In particular, the neutron-rich $Z = 72$–76, $N \approx 116$ region, close to ^{188}Hf, is predicted to be strongly favoured [138, 139], and similarly favoured is the $Z \approx 110$, $N \approx 156$ region, close to ^{266}Ds [140]. Furthermore, there are predictions of superdeformed high-K states in neutron-deficient lead and polonium isotopes [141], and also oblate superdeformed high-K states in $Z \geqslant 120$ superheavy nuclei [142, 143].

As with spin-trap and seniority isomers, the sensitivity provided also by K isomers for the study of exotic nuclei is valuable in the context of r-process nucleosynthesis. One of the challenges for deformed nuclei is to understand the enhanced elemental abundance in the $A \approx 160$ region, the so-called rare-earth element peak [144]. Recent experimental studies [145–147] have exploited K isomers in this neutron-rich region to reveal excited-state structures that help to understand the shell effects associated with the evolution of strong quadrupole (β_2) deformation and the possibility of β_6 effects, but such studies are still at an early stage.

5. Isomers at the atomic-nuclear interface

Aside of their nuclear structure interest, isomers can interact with their atomic environment in unusual ways that may open up novel possibilities [148–154]. It is notable that isomers offer different opportunities compared to nuclear ground states. While unstable (radioactive) ground states can transform by β decay, and sometimes by α decay, fission and proton decay, isomers can also decay electromagnetically, by γ-ray and conversion-electron emission, which is unavailable to ground states. Therefore, the electromagnetic manipulation of isomers is of particular interest.

For example, isomers can store large amounts of energy. If an efficient way could be found to release that energy in a controlled manner, then a type of nuclear 'battery' could be constructed. One option would be for the energy release to be induced by externally applied radiation, and in this respect much attention has been given to the $K^\pi = 9^-$, $T_{1/2} > 4.5 \times 10^{16}$ years isomer of ^{180}Ta [41, 155, 156], and the $K^\pi = 16^+$, $T_{1/2} = 31$ years isomer of ^{178}Hf [157–159]. This kind of challenge is, of course, open to all isomer types. Furthermore, another option could be to exploit the NEET (nuclear excitation by electronic transition) or NEEC (nuclear excitation by electron capture) processes. While the former was observed through excitation of the 1.9 ns first excited state of ^{197}Au by Kishimoto *et al* [160] in 2000, it is only recently that NEEC has been reported by Chiara *et al* [161], through induced depopulation of the $T_{1/2} = 7$ h isomer of ^{93}Mo, although the precise mechanism is not clear [162]. Further optimisation of the experimental conditions should be possible.

A special feature of the utility of isomers for these studies is illustrated by ^{93m}Mo. Here, a 5 keV, $E2$ excitation from the 2.4 MeV isomer enables the rapid release of the full isomer energy, including a 1.5 MeV γ ray. Although this is also emitted in the spontaneous decay of the isomer, there is a 268 keV γ-ray emission that is unique to the induced isomer decay, providing a clear signal that is distinct from any x-ray background [161]. It is one of the problems with the interpretation of the ^{178}Hf induced isomer decay that no such low-energy $E1$, $M1$ or $E2$ excitation pathway has been identified, although there is the possibility of a 126 keV, K-allowed $M2$ excitation that could enable the isomer energy to be released [163].

The involvement of atomic processes in isomer depopulation can also be important in astrophysical environments (see, for example, [153, 154]) and in this context there are several long-lived, two-quasiparticle isomers in odd–odd nuclides that provide valuable probes of those environments. Examples include ^{180m}Ta ($T_{1/2} > 4.5 \times 10^{16}$ years) and ^{186m}Re ($T_{1/2} = 2 \times 10^5$ years) and brief summaries of their roles can be found in the review of Dracoulis *et al* [59] (see also the even more recent publications [41, 164] and refs therein).

In the wider context, it is worthwhile to draw attention to the observation of superradiant decay (cooperative spontaneous emission of photons) from the 98 ns isomer of ^{57}Fe [165], excited by 14 keV synchrotron radiation. Furthermore, perhaps as a step towards a γ-ray laser, the generation of coherent γ radiation from a Bose–Einstein condensate of ^{135}Cs isomers ($T_{1/2} = 53$ m, 1.6 MeV) at ~100 nK has been proposed [166], without the need for externally applied radiation, except for the isomer production itself.

Finally, it is appropriate to mention recent work on the lowest-energy isomer of all, the 8.3 eV, $K^\pi = 3/2^+$ isomer of ^{229}Th [42], where the first direct detection of its decay has been achieved [167], as well as the first measurement of the

neutral-atom half-life of 7 μs [43]. The exceptionally low isomer energy leads to the expectation that its half-life will be particularly sensitive to the atomic environment [168], and there could be the possibility to construct an ultra-stable nuclear clock [169].

6. Conclusion

The properties of nuclear isomers have been introduced from an historical perspective. For a hundred years, isomers have been testing and stimulating concepts of nuclear structure, revealing features of both the individual-particle and collective degrees of freedom. Isomers continue to be pivotal in contemporary nuclear research, whether in their own right or through the access that they provide to remote regions of the nuclear landscape. Moreover, isomers offer unique opportunities at the atomic−nuclear interface, with the potential for further remarkable discoveries.

Acknowledgments

This work benefits from recent reviews and many discussions. In particular, George Dracoulis, Paddy Regan, Furong Xu, Yuri Litvinov, Filip Kondev, Rod Clark, Hubert Grawe and Magdalena Górska are thanked for their long-standing support. The research is funded in part by the United Kingdom Science and Technology Facilities Council under grant no. ST/L005743/1.

References

[1] Grinberg A P 1980 *Sov. Phys.—Usp.* **23** 848
[2] Soddy F 1917 *Nature* **99** 433
[3] Hahn O 1921 *Chem. Ber.* **54** 1131
[4] Fajans K and Göhring O 1913 *Naturwissenschaften* **1** 339
[5] Fry C and Thoennessen M 2013 *At. Data Nucl. Data Tables* **99** 345
[6] Gamow G 1934 *Phys. Rev.* **45** 728
[7] Fermi E 1934 *Nature* **133** 757
[8] Amaldi E, d'Agostino O and Segrè E 1934 *Ric. Sci.* **2** 9–10
[9] Szilard L and Chalmers T A 1935 *Nature* **135** 98
[10] Kurchatov B V, Kurchatov I, Myssowski L and Roussinow L 1935 *C. R.* **200** 1201
[11] von Weizsäcker C F 1936 *Naturewissenschaften* **24** 813
[12] Feather N and Bretscher E 1938 *Proc. R. Soc.* A **165** 530
[13] Feenberg E 1949 *Phys. Rev.* **75** 320
[14] Mayer M G 1949 *Phys. Rev.* **75** 1969
[15] Haxel O, Jensen J H D and Suess H E 1949 *Phys. Rev.* **75** 1766
[16] Goldhaber M and Sunyar A W 1951 *Phys. Rev.* **83** 906
[17] Goldhaber M and Hill R D 1952 *Rev. Mod. Phys.* **24** 179
[18] Weart S R 1983 Discovery of nuclear fission *Contribution to Otto Hahn and the Rise of Nuclear Physics* (*University of Western Ontario Series in Philosophy of Science*) ed W R Shea vol 22 (Dordrecht: Reidel)
[19] Bethe H A 1937 *Rev. Mod. Phys.* **9** 69
[20] Blatt J M and Weisskopf V F 1952 *Theoretical Nuclear Physics* (New York: Wiley)
[21] Firestone R B and Shirley V S (ed) 1996 *Table of Isotopes* 8th edn (New York: Wiley)
[22] Hahn O and Strassmann F 1939 *Naturwissenschaften* **27** 11
[23] Meitner L and Frisch O R 1939 *Nature* **143** 239
[24] Alaga G, Alder K, Bohr A and Mottelson B R 1955 *Mat. Phys. Medd. Dan. Vid. Selsk.* **29** 9
[25] Chu T C 1950 *Phys. Rev.* **79** 582
[26] Burson S B, Blair K W, Keller H B and Wexler S 1951 *Phys. Rev.* **83** 62
[27] Bohr A and Mottelson B R 1953 *Phys. Rev.* **90** 717
[28] Polikanov S M, Druin V A, Karnaukhov V A, Mikheev V L, Pleve A A, Skobelev N K, Ter-Akopyan G M and Fomichev V A 1962 *Z. Eksp. Teoret. Fiz.* **42** 1464
Polikanov S M, Druin V A, Karnaukhov V A, Mikheev V L, Pleve A A, Skobelev N K, Ter-Akopyan G M and Fomichev V A 1962 *Sov. Phys.—JETP* **15** 1016
[29] Flerov G N and Polikanov S M 1964 *C. R. Cong. Int. Phys. Nucl.* **1** 407
[30] Metag V, Habs D and Specht H J 1980 *Phys. Rep.* **65** 1
[31] Bjørnholm S and Lynn J E 1980 *Rev. Mod. Phys.* **52** 725
[32] Singh B, Zywina R and Firestone R B 2002 *Nucl. Data Sheets* **97** 241
[33] Heyde K and Wood J L 2011 *Rev. Mod. Phys.* **83** 1467
[34] Smith M B, Walker P M, Ball G C, Carroll J J, Garrett P E, Hackman G, Propri R, Sarazin F and Scraggs H C 2003 *Phys. Rev.* C **68** 031302(R)
[35] Seren L, Friedlander H N and Turkel S H 1947 *Phys. Rev.* **72** 888
[36] Helmer R G, Greenwood R C and Reich C W 1971 *Nucl. Phys.* A **168** 449
[37] Audi G, Kondev F G, Wan M, Huang W J and Naimi S 2017 *Chin. Phys.* C **41** 030001
[38] Kondev F G, Dracoulis G D and Kibédi T 2015 *At. Data Nucl. Data Tables* **103–104** 50
Kondev F G, Dracoulis G D and Kibédi T 2015 *At. Data Nucl. Data Tables* **105–106** 105 (erratum)
[39] Patel Z *et al* 2016 *Phys. Lett.* B **753** 182
[40] Sletten G, Metag V and Liukkonen E 1976 *Phys. Lett.* B **60** 153
[41] Lehnert B, Hult M, Lutter G and Zuber K 2017 *Phys. Rev.* C **95** 044306
[42] Seiferle B *et al* 2019 *Nature* **573** 243
[43] Seiferle B, von der Wense L and Thirolf P G 2017 *Phys. Rev. Lett.* **118** 042501
[44] Gjørup N L, Bentley M A, Fabricius B, Holm A, Sharpey-Schafer J F, Sletten G and Walker P M 1990 *Z. Phys.* A **337** 353
[45] Broda R *et al* 2017 *Phys. Rev.* C **95** 064308
[46] Jackson K P, Cardinal C U, Evans H C, Jelley N A and Cerny J 1970 *Phys. Lett.* B **33** 281
[47] Cerny J, Esterl J E, Gough R A and Sextro R G 1970 *Phys. Lett.* B **33** 284
[48] Peker L K, Volmyansky E I, Bunakov V E and Oglobin S G 1971 *Phys Lett.* B **36** 547
[49] Bugrov V P, Bunakov V E, Kadmenskii S G and Furman V I 1985 *Sov. J. Nucl. Phys.* **42** 34
[50] Yuan C *et al* 2016 *Phys. Lett.* B **762** 237
[51] de Voigt M J A, Dudek J and Szymański Z 1983 *Rev. Mod. Phys.* **55** 949
[52] Heyde K, Van Isacker P, Waroquier M, Wood J L and Meyer R A 1983 *Phys. Rep.* **102** 291
[53] Wood J L, Heyde K, Nazarewicz W, Huyse M and van Duppen P 1992 *Phys. Rep.* **215** 101
[54] Walker P M and Dracoulis G D 1999 *Nature* **399** 35
[55] Walker P M and Dracoulis G D 2001 *Hyperfine Interact.* **135** 83
[56] Jain A K, Maheshwari B, Garg S, Patial M and Singh B 2015 *Nucl. Data Sheets* **128** 1
[57] Heyde K and Wood J L 2016 *Phys. Scr.* **91** 083008

[58] Walker P M and Xu F R 2016 *Phys. Scr.* **91** 013010
[59] Dracoulis G D, Walker P M and Kondev F G 2016 *Rep. Prog. Phys.* **79** 076301
[60] Ackermann D 2015 *Nucl. Phys.* A **944** 376
[61] Ackermann D and Theisen Ch 2017 *Phys. Scr.* **92** 083002
[62] Britt H C 1973 *At. Data Nucl. Data Tables* **12** 407
[63] Vandenbosch R 1977 *Ann. Rev. Nucl. Sci.* **27** 1
[64] Hall H L and Hoffman D C 1992 *Annu. Rev. Nucl. Part. Sci.* **42** 147
[65] Thirolf P G and Habs D 2002 *Prog. Part. Nucl. Phys.* **49** 325
[66] Myers W D and Swiatecki W J 1966 *Nucl. Phys.* **81** 1
[67] Brack M, Damgaard J, Jensen A S, Pauli H C, Strutinsky V M and Wong C Y 1972 *Rev. Mod. Phys.* **44** 320
[68] Schirmer J, Gerl J, Habs D and Schwalm D 1989 *Phys. Rev. Lett.* **63** 2196
[69] Kantele J *et al* 1984 *Phys. Rev.* C **29** 1693
[70] Chinn C R, Berger J-F, Gogny D and Weiss M S 1992 *Phys. Rev.* C **45** 1700
[71] Delaroche J-P, Girod M, Goutte H and Libert J 2006 *Nucl. Phys.* A **771** 103
[72] Möller P, Sierk A J, Ichikawa T, Iwamoto A, Bengtsson R, Uhrenholt H and Åberg S 2009 *Phys. Rev.* C **79** 064304
[73] Lu B-N, Zhao E-G and Zhou S-G 2012 *Phys. Rev.* C **85** 011301
[74] Koh M-H, Bonneau L, Quentin P, Hao T V N and Wigiran H 2017 *Phys. Rev.* **95** 014315
[75] Oberstedt A, Oberstedt S, Gawrys M and Kornilov N 2007 *Phys. Rev. Lett.* **99** 042502
[76] Limkilde P and Sletten G 1973 *Nucl. Phys.* A **199** 504
[77] Liu H L, Xu F R, Sun Y, Walker P M and Wyss R 2011 *Eur. Phys. J.* A **47** 135
[78] Möller P, Sierk A J, Bengtsson R, Sagawa H and Ichikawa T 2009 *Phys. Rev. Lett.* **103** 212501
Möller P, Sierk A J, Bengtsson R, Sagawa H and Ichikawa T 2012 *At. Data Nucl. Data Tables* **98** 149
[79] Andreyev A N *et al* 2000 *Nature* **405** 430
[80] Kramp J, Habs D, Kroth R, Music M, Schirmer J and Schwalm D 1987 *Nucl. Phys.* A **474** 412
[81] Henderson J, Jenkins D G, Davies P J, Alcorta M, Carpenter M P, Kay B P, Lister C J and Zhu S 2014 *Phys. Rev.* C **89** 064307
[82] Walker P M, Litvinov Yu A and Geissel H 2013 *Int. J. Mass Spectrom.* **349–350** 247
[83] Dracoulis G D, Byrne A P, Baxter A M, Davidson P M, Kibédi T, McGoram T R, Bark R A and Mullins S M 1999 *Phys. Rev.* C **60** 014303
[84] Campbell P, Moore I D and Pearson M R 2016 *Prog. Part. Nucl. Phys.* **86** 127
[85] Krane K S 1998 *Introductory Nuclear Physics* (New York: Wiley)
[86] Podolyák Zs *et al* 2009 *Phys. Lett.* B **672** 116
[87] Steer S J *et al* 2011 *Phys. Rev.* C **84** 044313
[88] Kondev F G 2005 *Nucl. Data Sheets* **105** 1
[89] Kondev F G 2007 *Nucl. Data Sheets* **108** 365
[90] Singh B 2007 *Nucl. Data Sheets* **108** 79
[91] Xiaolong H and Zhou Chunmei Z 2005 *Nucl. Data Sheets* **104** 283
[92] Racah G 1943 *Phys. Rev.* **63** 367
[93] Talmi I 1993 *Simple Models of Complex Nuclei* (New York: Harwood Academic)
[94] Mach H *et al* 2017 *Phys. Rev.* C **95** 014313
[95] Baglin C M 2012 *Nucl. Data Sheets* **113** 2187
[96] Abriola D and Sonzongi A A 2006 *Nucl. Data Sheets* **107** 2423
[97] Park J *et al* 2017 *Phys. Rev.* C **96** 044311
[98] Blazhev A *et al* 2004 *Phys. Rev.* C **69** 064304
[99] Gottardo A *et al* 2012 *Phys. Rev. Lett.* **109** 162502
[100] Shamsuzzoha Basunia M 2014 *Nucl. Data Sheets* **121** 561
[101] Van Isacker P 2011 *J. Phys.: Conf. Ser.* **322** 012003
[102] Simpson G S *et al* 2014 *Phys. Rev. Lett.* **113** 132502
[103] Sonzongi A A 2004 *Nucl. Data Sheets* **103** 1
[104] Chiara C J *et al* 2011 *Phys. Rev.* C **84** 037304
[105] Arima A and Ichimura M 1996 *Prog. Theor. Phys.* **36** 296
[106] Jain A K and Maheswari B 2017 *Phys. Scr.* **92** 074004
[107] Iskra L W *et al* 2014 *Phys. Rev.* C **89** 044324
[108] Zhang C T *et al* 2000 *Phys. Rev.* C **62** 057305
[109] Maheswari B and Jain A K 2016 *Phys. Lett.* B **753** 122
[110] Fornal B *et al* 2001 *Phys. Rev. Lett.* **87** 212501
[111] Steer S J *et al* 2008 *Phys. Rev.* C **78** 061302
[112] Jungclaus A *et al* 2007 *Phys. Rev. Lett.* **99** 132501
[113] Watanabe H *et al* 2013 *Phys. Rev. Lett.* **111** 152501
[114] Martinez-Pinedo G and Langanke K 1999 *Phys. Rev. Lett.* **83** 4502
[115] Gallagher C J 1960 *Nucl. Phys.* **16** 215
[116] Rusinov L I 1961 *Usp. Fiz. Nauk.* **73** 615
Rusinov L I 1961 *Sov. Phys.—Usp.* **4** 282
[117] Löbner K E G 1968 *Phys. Lett.* B **26** 369
[118] Stephens F S 1975 *Rev. Mod. Phys.* **47** 43
[119] Frauendorf S 2001 *Rev. Mod. Phys.* **73** 463
[120] Dracoulis G D *et al* 2009 *Phys. Rev.* C **79** 061303(R)
[121] Bengtsson T, Broglia R A, Vigezzi E, Barranco F, Dönau F and Zhang J Y 1989 *Phys. Rev. Lett.* **62** 2448
[122] Narimatsu K, Shimizu Y R and Shizuma T 1996 *Nucl. Phys.* A **601** 69
[123] Crowell B *et al* 1996 *Phys. Rev.* C **53** 1173
[124] Walker P M *et al* 1997 *Phys. Lett.* B **408** 42
[125] Walker P M 2017 *Phys. Scr.* **92** 054001
[126] Dracoulis G D *et al* 2006 *Phys. Rev. Lett.* **79** 122501
[127] Chen F-Q, Liu Y-X, Sun Y, Walker P M and Dracoulis G D 2012 *Phys. Rev.* C **85** 024324
[128] Chowdhury P *et al* 1988 *Nucl. Phys.* A **485** 136
[129] Dracoulis G D *et al* 2005 *Phys. Rev.* C **71** 044326
Dracoulis G D *et al* 2006 *Phys. Rev.* C **73** 019901(E) (erratum)
[130] Tandel S K *et al* 2006 *Phys. Rev.* C **73** 044306
[131] Gjørup N L, Walker P M, Sletten G, Bentley M A, Fabricius B and Sharpey-Schafer J F 1995 *Nucl. Phys.* A **582** 369
[132] Jain K, Burglin O, Dracoulis G D, Fabricius B, Rowley N and Walker P M 1995 *Nucl. Phys.* A **591** 61
[133] Xu F R, Walker P M, Sheikh J A and Wyss R 1998 *Phys. Lett.* B **435** 257
[134] Sun Y, Zhou X R, Long G L, Zhao E G and Walker P M 2004 *Phys. Lett.* B **589** 83
[135] Cullen D M *et al* 1999 *Phys. Rev.* C **60** 064301
[136] Xu F R, Zhao E G, Wyss R and Walker P M 2004 *Phys. Rev. Lett.* **92** 252501
[137] Liu H L, Xu F R, Walker P M and Bertulani C A 2011 *Phys. Rev.* C **83** 011303(R)
[138] Liu H L, Xu F R, Walker P M and Bertulani C A 2011 *Phys. Rev.* C **83** 067303
[139] Xu F R, Walker P M and Wyss R 2000 *Phys. Rev.* C **62** 014301
[140] Liu H L, Walker P M and Xu F R 2014 *Phys. Rev.* C **89** 044304
[141] Shi Y, Xu F R, Walker P M and Dracoulis G D 2012 *Phys. Rev.* C **85** 064304
[142] Jachimowicz P, Kowal M and Skalski J 2011 *Phys. Rev.* C **83** 054302
[143] Liu H L 2013 *Commun. Theor. Phys.* **60** 577
[144] Surman R, Engel J, Bennett J R and Meyer B S 1997 *Phys. Rev. Lett.* **79** 1809
[145] Patel Z *et al* 2014 *Phys. Rev. Lett.* **113** 262502
[146] Ideguchi E *et al* 2016 *Phys. Rev.* C **94** 064322
[147] Watanabe H *et al* 2016 *Phys. Lett.* B **760** 641
[148] Baldwin G C and Solem J C 1997 *Rev. Mod. Phys.* **69** 1085

[149] Matinyan S 1998 *Phys. Rep.* **298** 199
[150] Aprahamian A and Sun Y 2005 *Nat. Phys.* **1** 81
[151] Carroll J J 2007 *Nucl. Instrum. Methods Phys. Res.* B **261** 960
[152] Rivlin L A 2007 *Quantum Electron.* **37** 723
[153] Gosselin G, Méot V and More P 2007 *Phys. Rev.* C **76** 044611
[154] Gosselin G, Morel P and Mohr P 2010 *Phys. Rev.* C **81** 055808
[155] Belic D *et al* 1999 *Phys. Rev. Lett.* **83** 5242
[156] Walker P M, Dracoulis G D and Carroll J J 2001 *Phys. Rev.* C **64** 061302(R)
[157] Collins C B *et al* 1999 *Phys. Rev. Lett.* **82** 695
[158] Carroll J J *et al* 2009 *Phys. Lett.* B **679** 203
[159] Kirischuk V I, Ageev V A, Dovbnya A M, Kandybei S S and Ranyuk Yu M 2015 *Phys. Lett.* B **750** 89
[160] Kishimoto S, Yoda Y, Seto M, Kobayashi Y, Kitao S, Haruki R, Kawauchi T, Fukutani K and Okano T 2000 *Phys. Rev. Lett.* **85** 1831
[161] Chiara C J *et al* 2018 *Nature* **554** 216
[162] Wu Y, Keitl C H and Pálffy A 2019 *Phys. Rev. Lett.* **122** 212501
[163] Carroll J J 2004 *Laser Phys. Lett.* **1** 275
[164] Matters D A *et al* 2017 *Phys. Rev.* C **96** 014318
[165] Röhlsberger R, Schlage K, Sahoo B, Couet S and Rüffer R 2010 *Science* **328** 1248
[166] Marmugi L, Walker P M and Renzoni F 2018 *Phys. Lett.* B **777** 281
[167] von der Wense L *et al* 2016 *Nature* **533** 47
[168] Tkalya E V 2018 *Phys. Rev. Lett.* **120** 122501
[169] Campbell C J, Radnaev A G, Kuzmich A, Dzuba V A, Flambaum V V and Derevianko A 2012 *Phys. Rev. Lett.* **108** 120802